

# Implementation and Validation of an IEEE 802.11ah Module for ns-3

Le Tian\*, Sébastien Deronne†, Steven Latré\*, Jeroen Famaey\*

\* Department of Mathematics and Computer Science, University of Antwerp – iMinds, Belgium  
{le.tian, steven.latre, jeroen.famaey}@uantwerpen.be

† Nokia, Belgium  
sebastien.deronne@gmail.com

## ABSTRACT

IEEE 802.11ah or HaLow is a new Wi-Fi standard for sub-1Ghz communications, aiming to address the major challenges of the Internet of Things: connectivity among a large number of power-constrained stations deployed over a wide area. Existing research on the performance evaluation of 802.11ah is generally based on analytical models, which does not accurately represent real network dynamics and is hard to adjust to different network conditions. To address this hiatus, we implemented the 802.11ah physical and MAC layer in the ns-3 network simulator, which, compared to analytical models, more closely reflects actual protocol behavior and can more easily be adapted to evaluate a broad range of network and traffic conditions. In this paper, we present the details of our implementation, including a sub-1Ghz physical layer model and several novel MAC layer features. Moreover, simulations based on the implemented model are conducted to evaluate performance of the novel features of IEEE 802.11ah.

## CCS Concepts

•Networks → Wireless access networks; •Computing methodologies → Model development and analysis; Simulation evaluation;

## Keywords

IEEE 802.11ah, Wi-Fi HaLow, ns-3, Fast Association, Restricted Access Window

## 1. INTRODUCTION

The Internet of Things (IoT) consists of millions of constrained devices addressable over the Internet. Existing low-power wireless network technologies for connecting such devices can be categorized into two groups: (i) wireless personal area networking (WPAN) technologies that provide

Permission to make digital or hard copies of all or part of this work for personal or classroom use is granted without fee provided that copies are not made or distributed for profit or commercial advantage and that copies bear this notice and the full citation on the first page. Copyrights for components of this work owned by others than the author(s) must be honored. Abstracting with credit is permitted. To copy otherwise, or republish, to post on servers or to redistribute to lists, requires prior specific permission and/or a fee. Request permissions from [permissions@acm.org](mailto:permissions@acm.org).

WNS3, June 15 - 16, 2016, Seattle, WA, USA

© 2016 Copyright held by the owner/author(s). Publication rights licensed to ACM. ISBN 978-1-4503-4216-2/16/06...\$15.00

DOI: <http://dx.doi.org/10.1145/2915371.2915372>

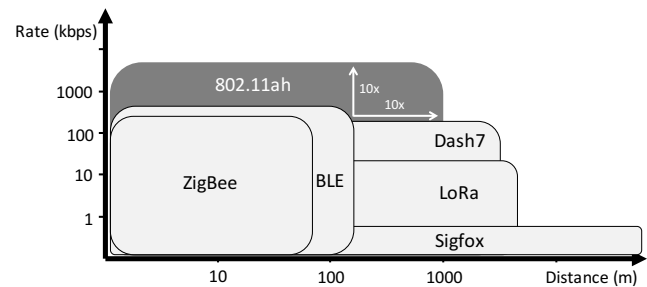


**Figure 1: Position of IEEE 802.11ah compared to existing WPAN and LPWAN technologies, promising considerably extended range compared to WPAN and higher bitrate than LPWAN.**

connectivity up to tens of meters (e.g., ZigBee, Bluetooth Low Energy) and (ii) low-power wide-area networking (LP-WAN) technologies that offer an extended range up to several kilometers but sacrifice in terms of throughput (e.g., LoRaWAN, Sigfox, DASH-7). As such, a gap still exists for a low-power communication technology that offers both extended range and higher throughput.

The new IEEE 802.11ah standard, marketed as Wi-Fi HaLow, fills this gap, combining the advantages of Wi-Fi and low-power communication technologies (cf. Figure 1). IEEE 802.11ah is a wireless communication PHY and MAC layer protocol that operates in the unlicensed sub-1Ghz frequency bands (e.g., 863–868 Mhz in Europe and 902–928 Mhz in North-America). It was designed to provide communications at a range of up to 1 kilometer while maintaining a data rate of 150 Kbps, offering a much greater coverage than existing WPAN and considerably higher throughput than LP-WAN technologies. In the MAC layer, 802.11ah introduces mechanisms such as hierarchical organization, short MAC header, fast association, restricted access window (RAW), traffic indication map (TIM) segmentation and target wake time (TWT) to support densely deployed energy-constrained stations.

Even though the IEEE 802.11ah standard has only been officially released since January 2016, researchers have been investigating it already for a few years. Several recent studies investigate physical layer aspects of IEEE 802.11ah specifically and sub-1Ghz communications generally [5, 3, 2, 4]. Hazmi et al. [5] study link budget, achievable data rate and

**Table 1: 802.11ah MCSs for 1, 2 MHz, NSS=1, GI=8  $\mu$ s.**

MCS Index	Modulation	Coding rate	Data rate (Kbps)	
			1 Mhz	2 Mhz
0	BPSK	1/2	300	650
1	QPSK	1/2	600	1300
2	QPSK	3/4	900	1950
3	16-QAM	1/2	1200	2600
4	16-QAM	3/4	1800	3900
5	64-QAM	2/3	2400	5200
6	64-QAM	3/4	2700	5850
7	64-QAM	5/6	3000	6500
8	256-QAM	3/4	3600	7800
9	256-QAM	5/6	4000	Not valid
10	BPSK	1/2 with 2x repetition	150	Not valid

the influence of packet size in different scenarios. Moreover, a few studies of the IEEE 802.11ah physical layer have been performed using an implementation based on Software Defined Radios (SDRs) [3, 2, 4]. Current research on the MAC layer of 802.11ah mainly focuses on performance of the RAW mechanism [11, 7, 16, 12, 13, 9, 8]. Nearly all of this research is based on analytical modelling of the saturated network state. Such models do not accurately capture real network behavior and are hard to adapt to non-saturated network conditions. Only Raeesi et al. [12] performed actual simulations using OMNeT++.

To address this hiatus, we have implemented the 802.11ah standard in the ns-3 network simulator. Our implementation builds upon existing 802.11 implementations in ns-3 and extends them with a physical layer model for sub-1GHz radio communications and a subset of the new MAC layer features of the standard. The implementation is modular, allowing it to be easily extended with additional 802.11ah-specific features. Moreover, it has been made available as open source for other researchers to experiment with<sup>1</sup>.

Our simulation model has several benefits compared to the OMNeT++ model implemented by Raeesi et al. [12]. Specifically, their RAW implementation does not support grouping. Moreover, we have implemented the fast association and two-stage back-off mechanisms. Finally, their implementation, in contrast to ours, is not publicly available.

The contributions of this paper are twofold. First, we outline our implementation, its features, and its integration into ns-3. Second, we have conducted an in-depth simulation study to validate our implementation.

The remainder of this paper is structured as follows. Section 2 provides an overview of the most prominent 802.11ah features, both on the PHY and MAC layer. Details on the ns-3 implementation model are provided in Section 3. In Section 4, we validate both the physical and MAC layer of the implemented model. The planned future extensions to our implementation are detailed in Section 5. Finally, conclusions are discussed in Section 6.

## 2. OVERVIEW OF THE IEEE 802.11AH

IEEE 802.11ah operates at sub-1GHz, supporting long

distance transmission, 8192 nodes connected to a single AP and high energy efficiency. These features make it an attractive standard for long-range IoT applications, such as sensor-based monitoring, smart meters and home automation. Throughout this section we highlight aspects of the standard that are important for our implementation. For a more detailed overview of the standard, the reader is referred to existing literature [6, 1].

### 2.1 PHY Layer

The IEEE 802.11ah PHY layer inherits characteristics from IEEE 802.11ac and adapts them to sub-1GHz frequencies. Its channel bandwidths range from 1 to 16 MHz, with 1 and 2 MHz support being mandatory. Operating at low frequency and narrow bandwidth allows it to transmit at longer ranges (up to 1 km or more in theory) with considerably less power consumption than traditional Wi-Fi technologies, which use frequencies in the 2.4 and 5 GHz bands.

For different data rates and bandwidths, 802.11ah utilizes different sets of modulation and coding schemes (MCSs), number of spatial streams (NSS) and duration of the guard interval (GI). Coding schemes include binary conventional coding (BCC), which is mandatory, as well as the optional low density parity check (LDPC). Table 1 lists data rates and their MCSs when GI and NSS are 8  $\mu$ s and 1 respectively for 1 and 2 MHz bandwidth.

### 2.2 MAC Layer

The MAC layer of IEEE 802.11ah consists of several novel features, such as fast association and authentication, RAW, TIM segmentation and TWT, aiming to address the requirements of dense IoT networks. Details of the those features are described as follows.

#### 2.2.1 Fast Authentication and Association

When an AP is deployed or after a power outage, a large number of stations are simultaneously trying to associate, this process could take a long time due to collisions. Two more effective fast authentication and association control mechanisms (i.e., centralized and distributed), are proposed for IEEE 802.11ah. In centralized authentication, the AP sets a threshold in authentication control elements attached to a beacon. When a station is initialized, it generates a random value from the interval [0, 1022] and send authentication/association requests to the AP if the random value is smaller than the threshold obtained from the received beacon, otherwise postpone authentication/association until the next beacon. The threshold should be adjusted dynamically by the AP to allow all stations to get associated eventually. Distributed authentication is based on the truncated binary exponential back-off, each beacon interval is divided into slots of equal duration, stations randomly select one slot to send their association request.

#### 2.2.2 Restricted Access Window (RAW)

The RAW mechanism aims to reduce collisions and improve throughput when hundreds or even thousands of stations are simultaneously contending for channel access. It restricts the number of stations that can simultaneously access the channel by splitting them into groups and only allowing stations that belong to a certain group to access the channel at specific times. Figure 2 schematically depicts how RAW works. Specifically, the airtime is split into intervals,

<sup>1</sup><https://www.uantwerpen.be/en/rg/mosaic/projects/ieee-802-11ah/>

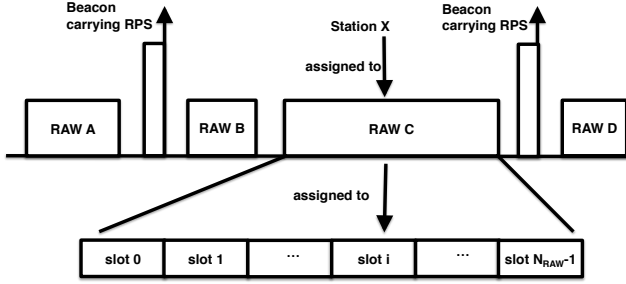


Figure 2: Schematic representation of the RAW mechanism.

each of which is assigned to one RAW group. Each interval is preceded by a beacon that carries a RAW parameter set (RPS) information element that specifies the stations that belong to the group, as well as the interval start time. Moreover, each RAW interval consists of one or more slots, over which the stations in the RAW group are split evenly. As such, the RPS also contains the number of slots, slot format and slot duration count sub-fields which jointly determine the RAW slot duration as follows:

$$D = 500 \mu s + C \times 120 \mu s \quad (1)$$

Where  $C$  represents slot duration count sub-field, which is either  $y = 11$  or  $y = 8$  bits long if the slot format sub-field is set to respectively 1 or 0. The number of slots field is  $14 - y$  bits long.

Different from previous IEEE 802.11 technologies, each station uses two back-off states of enhanced distributed channel access (EDCA) to manage transmission inside and outside its assigned RAW slot respectively. The first back-off function state is used outside RAW and the second is used inside RAW slots. For the first back-off state, the station suspends its back-off at the start of each RAW and stores the back-off states, then restores them and resumes back-off at the end of the RAW. For the second back-off state, stations start back-off with initial back-off state inside their own RAW slot, and disregard the back-off state at the end of their RAW slot. As shown in Figure 3, station 1 is inside the RAW group and assigned to slot 1, while station 2 is not included in this RAW group. Therefore, station 1 uses the first back-off state outside its RAW slot period and the second back-off state inside its RAW slot, while station 2 only uses the first back-off state outside the RAW group period and goes into a sleep state inside the RAW group period.

### 2.2.3 Power Saving Mechanisms

In the current 802.11 standards, beacons trigger power saving (PS) station contention for the channel, which is the bottleneck of the whole power management framework since stations have to wake up to listen to every beacon. IEEE 802.11ah introduces the TIM segmentation mechanism to split information transmitted in the TIM into several segments and transmit them separately. In addition to using TIM beacons for station-level signaling, as shown in Figure 4, it also uses delivery traffic indication map (DTIM) beacons for TIM group-level signaling. The AP uses the DTIM beacon to broadcast to stations which TIM segments have pending data, stations only need wake up to listen to

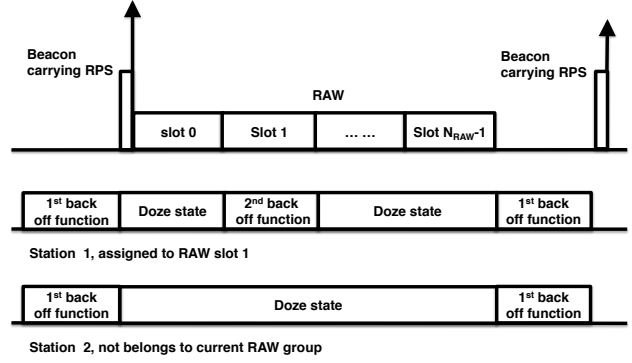


Figure 3: Back-off procedure for the IEEE 802.11ah RAW mechanism.

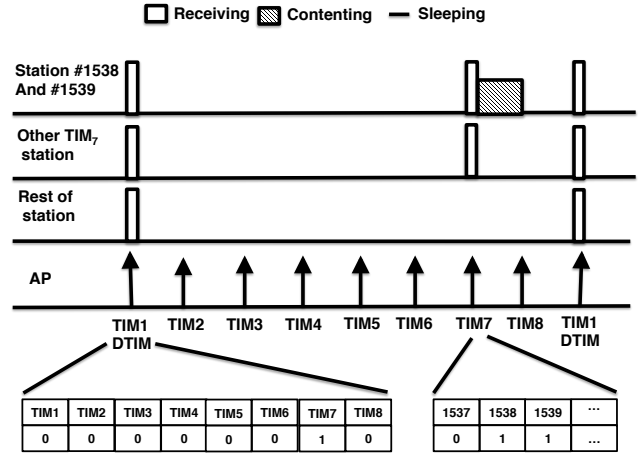


Figure 4: Example of the TIM segmentation mechanism (source: Adame et al. [1]).

their corresponding TIM beacon, thus they can maintain a longer power-saving state. Power consumption can be further reduced by TWT for stations transmitting data rarely. TWT stations can negotiate a time slot with the AP when they should wake up to exchange frames, therefore they can stay in a power-saving state for very long periods of time during their TWT intervals.

## 3. IMPLEMENTATION

Currently, ns-3 comes with support for several IEEE 802.11 standards, including 802.11a, 802.11b, 802.11g, 802.11n and since recently 802.11ac. As Figure 5 shows, the components of the ns-3 Wi-Fi PHY and MAC models consist of 4 main components:

- WifiChannel: An analytical approximation of the physical medium over which data is transmitted (i.e., the air in case of Wi-Fi), consisting of propagation loss and delay models.
- WifiPhy: The PHY part of the protocol, takes care of sending and receiving frames and determining loss due to interference.
- MacLow: Implements RTS/CTS/DATA/ACK trans-

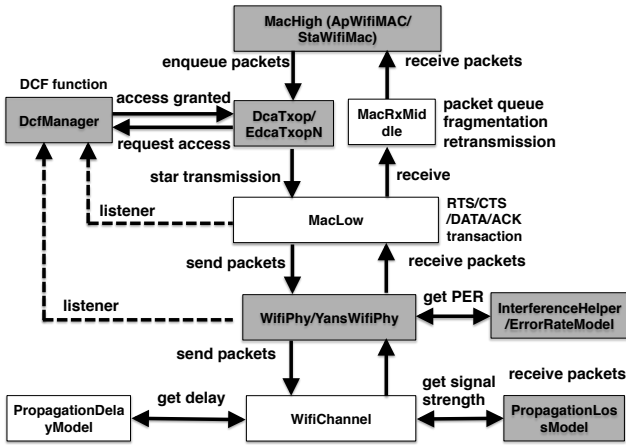


Figure 5: ns-3 Wi-Fi models and interactions; grey background denotes changed components in our implementation.

actions, the distributed coordination function (DCF) and enhanced distributed channel access (EDCA), packet queues, fragmentation, re-transmission and rate control.

- MacHigh: Implements management functions such as beacon generation, probing, association.

The remainder of this section outlines how we adapted the above models to support 802.11ah. Our implementation is based on ns-3 version 3.23.

### 3.1 PHY Layer

Our work in implementing 802.11ah PHY model focused on the components marked in Figure 5: InterferenceHelper, ErrorRateModel, WifiPhy, YansWifiPhy and PropagationLossModel.

#### 3.1.1 WifiPhy and YansWifiPhy

In the WifiPhy class, the modulation and coding schemes MCS0 to MCS9 for channel bandwidths 1, 2, 4, 8 and 16 Mhz (cf. Table 1) are defined, while MCS10 is currently not supported by our implementation. Moreover, header and preamble formats of IEEE 802.11ah as well as the way of calculating sending/receiving duration of the preamble, header and payload are implemented. The `ConfigureStandard()`, `WifiModeToMcs()`, and `McsToWifiMode()` functions in YansWifiPhy are modified to support the 802.11ah configuration and the conversion between Wi-Fi mode and MCS.

#### 3.1.2 InterferenceHelper and ErrorRateModel

Since 802.11ah defines new header formats, the `CalculatePlcpPayloadPer()` and `CalculatePlcpHeaderPer()` functions in the InterferenceHelper class are revised to calculate the length of received 802.11ah packets, which is required for the packet error rate calculation. Additionally, the `NistErrorRate` and `YansErrorRate` classes are modified to be capable of calculating the packet error rate of 802.11ah with support for the QAM256 modulation scheme. It is worth noting that YansErrorRate model is known to be too optimistic, while NistErrorRate model better matches experimental results according to Pei and Henderson [10].

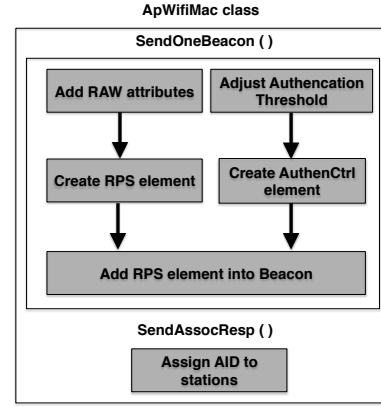


Figure 6: New functionality in ApWifiMac class.

#### 3.1.3 PropagationLossModel

This model determines the signal strength in the wireless medium based on the distance between sender and receiver. We implemented the indoor and outdoor propagation loss models for 802.11ah developed by Hazmi et al. [5]. They proposed two different outdoor models, one for macro deployments and one for pico or hotzone deployments. The macro deployment model assumes an antenna height of 15 meters above a rooftop, with the propagation loss (in dB) given as follows:

$$L(d) = 8 + 37.6 \log_{10}(d) + 21 \log_{10}\left(\frac{f}{900\text{MHz}}\right) \quad (2)$$

The pico deployment model is assumed to be at rooftop height, with the propagation loss (in dB) given as follows:

$$L(d) = 23.3 + 36.7 \log_{10}(d) + 21 \log_{10}\left(\frac{f}{900\text{MHz}}\right) \quad (3)$$

Finally, the indoor propagation loss model is the same as that of 802.11n, and consists of the free space loss (FSL) with a slope of 2 up to a breakpoint distance and a slope of 3.5 after this breakpoint:

$$L(d) = \begin{cases} 20 \log_{10}\left(\frac{4d\pi f}{c}\right) & d \leq d_{BP} \\ 20 \log_{10}\left(\frac{4d\pi f}{c}\right) + 35 \log_{10}\left(\frac{d}{d_{BP}}\right) & d > d_{BP} \end{cases} \quad (4)$$

With  $d$ ,  $f$ ,  $c$  and  $d_{BP}$  the transmit-receive distance in meters, carrier frequency, speed of light and breakpoint distance respectively.

### 3.2 MAC Layer

Among the new features of IEEE 802.11ah listed in Section 2, our simulator currently supports fast association and RAW, the implementation mainly focuses on the MacHigh, DcaTxop, EdcaTxopN and DcfManager components. The implementation of the power-saving features (e.g., TIM segmentation and TWT) is planned as future work.

#### 3.2.1 MacHigh

As shown in Figures 6 and 7, new functionality is added in both ApWifiMac and StaWifiMac in order to support fast association and RAW.

For the ApWifiMac class, RAW related attributes, as listed in Table 2, are added in order to allow user configuration.

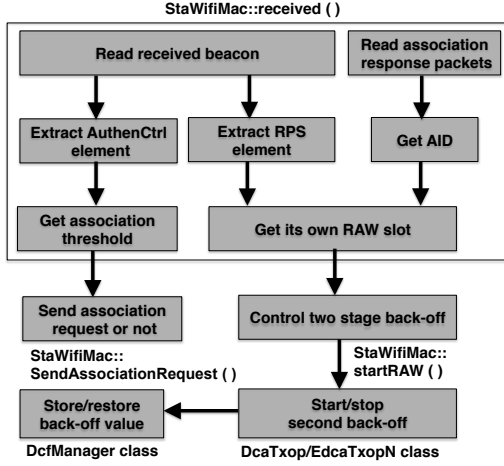


Figure 7: New functionality in StaWifiMac class.

Table 2: 802.11ah attributes in ApWifiMac class.

Parameter	Description
NRawGroupStas	Stations per RAW group
NRawStations	Stations supporting RAW
SlotFormat	Slot format
SlotDurationCount	Slot duration count
NRawSlotNum	Slots per RAW group

The RPS and AuthenCtrl elements, which carry RAW group and association information, are defined in a new classes, and are generated and attached to beacons based on the values of the newly defined attributes. A mechanism for adjusting the association threshold is implemented as well, to allow changing the threshold dynamically. Besides that, the AID assignment scheme is added in the `SendAssocResp()` function to allows the AP to assign an AID to stations during the association exchange.

For the StaWifiMac class, the station receives an association threshold and RAW information from the RPS and AuthenCtrl elements carried by the received beacon, and gets an AID from the association response packet in the `received()` function. Based on the association threshold, the station determines to send an association request or not. RAW information and the AID jointly determine the RAW slot stations belong to and control the two stage back-off, making sure stations are allowed to access the channel during their own RAW slot.

### 3.2.2 DcaTxopN, EdcaTxopN and DcfManager

The two stage back-off mechanism was implemented in the DcaTxop, EdcaTxopN and DcfManager classes, supporting both Quality of Service (QoS) and non-QoS data transmissions. The start and termination of the two stage back-off is managed by the DcaTxop and EdcaTxopN classes by sending instructions to the DcfManager class, which is modified to be able to store and restore back-off related values. Based on the instructions from the StaWifiMac class, stations start to contend for the channel in the appropriate slot with the corresponding back-off state. Additionally, the WifiRemoteStationManager class is modified as well to store and restore the re-transmission counter of the two back-off states.

Table 3: Default physical layer parameters used in our experiments.

Parameter	Value
Frequency	900 Mhz
Transmission power	0 dBm
Transmission gain	0 dB
Reception gain	3 dB
Noise Figure	3 dB
Coding method	BCC
Propagation loss model	Outdoor, macro [5]
Error Rate Model	NistErrorRate, YansErrorRate

Table 4: Default MAC layer parameters used in our experiments.

Parameter	Value
CWmin	15
CWmax	1023
AIFSN	3
Traffic access categories	AC_BE
Payload size	256 bytes
MAC header type	legacy header
RTS/CTS	not enabled
Beacon Interval	0.1 s
Cross slot boundary	enabled
Station distribution	randomly
Wi-Fi mode	MCS8, 2 Mhz
Rate control algorithm	constant

## 4. EVALUATION

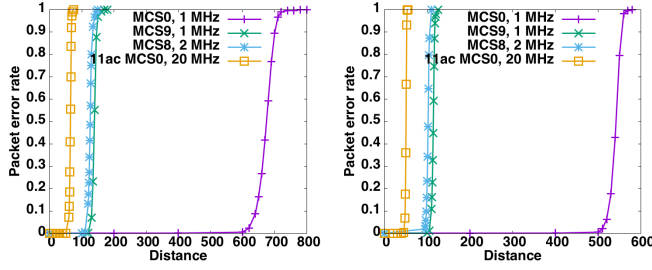
In this section we present and discuss our results obtained using the ns-3 implementation of IEEE 802.11ah. The simulation setup is described, and the implementation of the physical layer, fast association and RAW is validated.

### 4.1 Simulation Setup

We consider an IoT sensor-based monitoring scenario where a large number of battery-powered sensors send measurements to a back-end server (through the AP) at specific time intervals. Stations are deployed randomly within a 400 meter diameter around the AP. The default PHY and MAC layer parameters are shown in Tables 3 and 4 respectively. Note that these are the default parameter values, and some of them take different values in specific experiments (e.g., Wi-Fi mode), which is explicitly mentioned. Given the low-power nature of battery-powered sensors, transmission power is limited to 0 dBm. Like 802.11ac, 802.11ah uses forward error correction (FEC) schemes to improve transmission range. With the same physical parameters, we also test Wi-Fi mode MCS0 of 802.11ac, which has a data rate of 6.5 Mbps for bandwidth of 20 MHz.

### 4.2 Physical Layer

This section evaluates the physical layer packet error rate as a function of distance of different 802.11ah Wi-Fi modes for outdoor macro deployments, using the parameters defined in Table 3. Figure 8 shows the transmission range of different Wi-Fi modes. When YansErrorRateModel is used, IEEE 802.11ah can transmit over distances up to 640 m with a packet error rate below 10% and up to 670 m with an error rate below 50% using MCS0 with 1 Mhz bandwidth, which achieves data rates up to 300 kbps. Results also clearly show that using modes that provide higher data rate signifi-



(a) YansErrorRate Model (b) NistErrorRate Model

Figure 8: Packet error rate as a function of uplink distance with different ErrorRate Model for various IEEE 802.11ah Wi-Fi modes and compared to IEEE 802.11ac.

cantly reduces the maximum transmission distance. For example, MCS9 with 1 Mhz bandwidth and MCS8 with 2 Mhz bandwidth are capable of achieving data rate up to 4 Mbps and 7.8 Mbps respectively. They allow error-free transmission up to 130 and 110 m respectively. For comparison, IEEE 802.11ac only has a range of up to 60 m with a data rate of 6.5 Mbps and an error rate of 10% (at an equal 0 dBm transmission power). As indicated in Section 3.1, the transmission range becomes shorter when NistErrorRateModel is applied, around 150, 20 and 10 m are lost for Wi-Fi modes MCS0 with 1 Mhz, MCS9 with 1 Mhz and MCS8 with 2 Mhz bandwidth. It should be noted that the 1 km range promised by 802.11ah could potentially be realized using the MCS10 mode together with LDPC coding, since it is capable of bridging higher distances. This mode's implementation is left for future work.

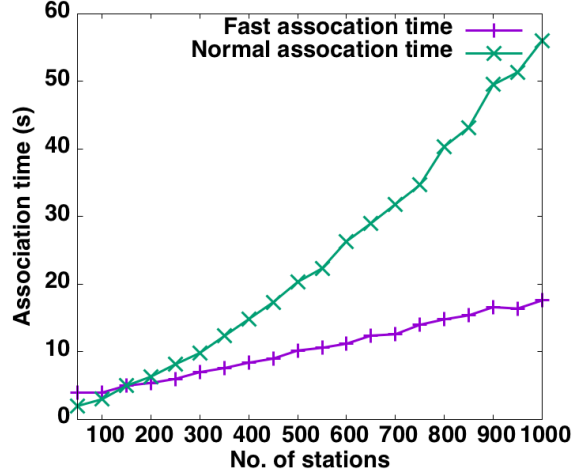


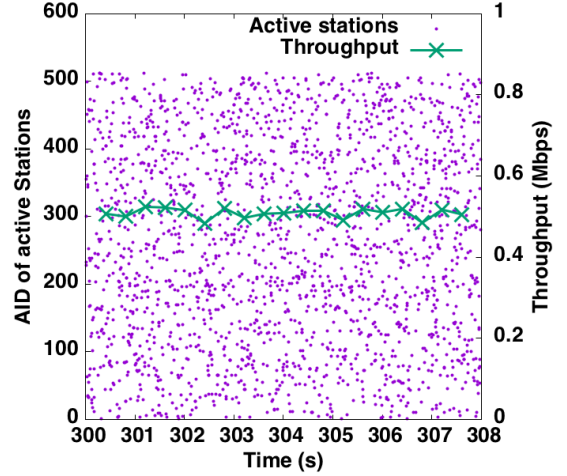
Figure 9: Association time comparison between normal association and fast association.

### 4.3 Fast Association Mechanism

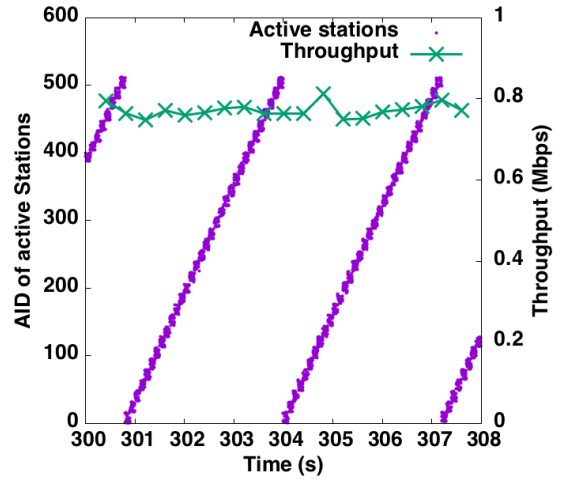
In this section, we evaluate the fast association mechanism for a varying number of stations. A threshold adaptation mechanism proposed by Wang [15] is adopted in this simu-

lation, in which the AP adjusts the association threshold dynamically based on its sending queue size. This results in increasing the threshold by 50 when the queue is smaller than 10, otherwise decreasing the threshold by 50. The result is depicted in Figure 9, which clearly reveals that fast association substantially decreases association time, especially for a large number of stations. It is quite straightforward since fewer stations are allowed to send association requests simultaneously, reducing the collision probability. Association performance could be further improved with more advanced threshold adaptation algorithms.

### 4.4 RAW Mechanism



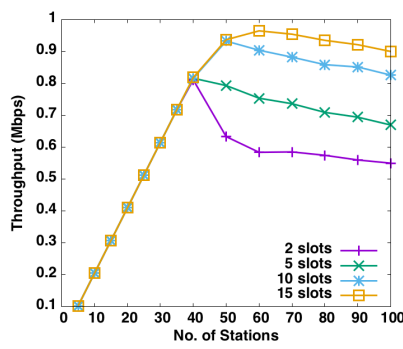
(a) Without RAW



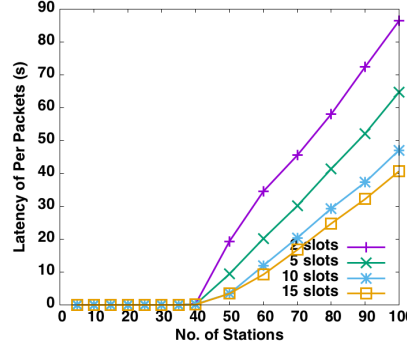
(b) With 32 RAW groups

Figure 10: Number of active stations and instantaneous throughput for a 512 station network.

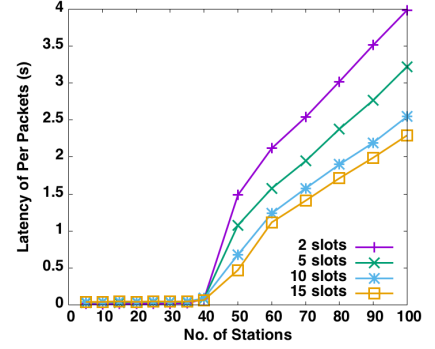
Figure 10 depicts the active stations (by AID) and throughput at each instant in time with and without the use of RAW. Figure 10a clearly shows that the channel is randomly utilized by stations all the time without the use of RAW. Due to the density of the network this results in many collisions and an average throughput of around 0.5 Mbps. In contrast,



(a) Throughput



(b) Latency(infinite queue)



(c) Latency(queue of 10-packets)

Figure 11: Throughput and latency for varying number of RAW slots.

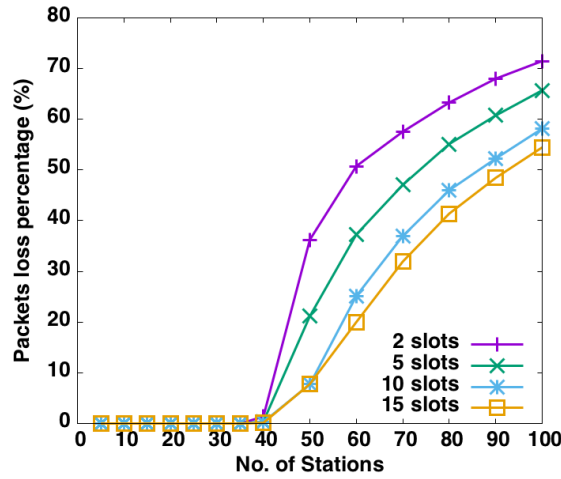


Figure 12: Packets loss with different number of RAW slots when the length of send queue is 10 packets.

Figure 10b clearly shows that the RAW mechanisms results in a more controlled channel access manner, only allowing contention among a limited number of stations. As a result, collision probability drops and the average throughput increases by 50% and becomes 0.75 Mbps.

Figure 11 aims to assess the influence of the number of RAW slots per group, as well as transmit buffer length on throughput and latency. The reader is referred to our previous work [14] for the impact of the number of RAW groups. There is a single RAW group, and each station sends one packet every 0.1 seconds to the AP with a random starting time. Due to the relatively small payload size, the maximum throughput that can be achieved using MCS8 with 2 Mhz bandwidth is around 1 Mbps. The network becomes congested when there are more than 50 stations transmitting. In the case of an infinite buffer, no packets are dropped, while packet loss for the case with a 10 packet buffer is shown in Figure 12.

Figure 11 clearly shows that the RAW slot parameter has no effect on performance for a small number of sta-

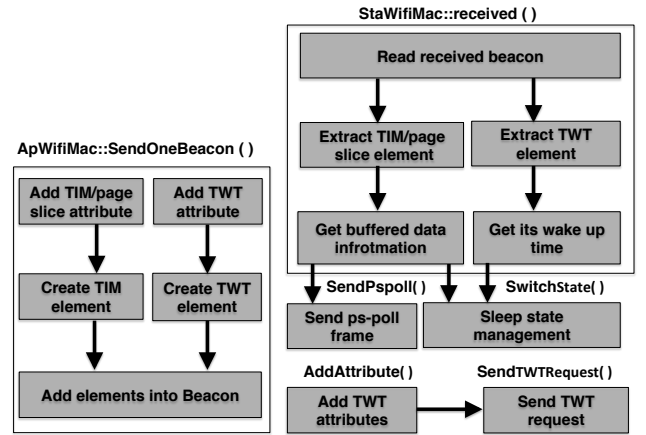


Figure 13: Future planned implementation of TIM segmentation and TWT.

tions. However, higher throughput and reduced latency can be achieved for more stations with a larger number of slots. This is because splitting stations into RAW slots reduces contention, and in turn collision probability and re-transmissions. However, it should be noted that very many slots could make the duration of slots too short to be enough for one packet to be successfully sent.

The use of an infinite transmit buffer obviously results in a considerable latency increase as congestion increases. On the other hand, a limited buffer space causes a considerable amount of packet loss. Finally, the fact that a higher number of RAW slots results in significantly less packet loss, again confirms that RAW reduces contention.

## 5. FUTURE IMPLEMENTATION PLANS

Our aim is to implement TIM segmentation and TWT in ns-3 in the near future. As shown in Figure 13, the implementation will focus on ApWifiMac and StaWifiMac. For the ApWifiMac class, TIM and TWT elements will be defined and attached to beacons according to the related attributes. For the StaWifiMac class, functionality such as reading TIM and TWT elements from received beacons,

sending ps-poll frames and managing sleep state indicated by the TIM and TWT elements, is going to be implemented. Since the TWT setup can be launched by both stations and the AP, TWT related attributes and sending TWT requests will also be implemented in the StaWifiMac class. Moreover, support for MCS10 Wi-Fi mode will be added by implementing LDPC coding with 2x repetition. On the longer term, we aim to support other features of 802.11ah, such as Relays and hierarchical RAW. Finally, work is in progress to include 802.11ah support in a future ns-3 official release.

## 6. CONCLUSION

This paper presents an implementation of the IEEE 802.11ah physical and MAC layer protocol for the ns-3 network simulator. The implementation and its integration into ns-3 are described in detail. Moreover, the implementation was evaluated, validated through simulation based on the implemented model. The evaluation confirmed a correct behavior of the fast association and RAW MAC-layer mechanisms. Moreover, 802.11ah is shown to be a promising wireless technology for densely deployed IoT applications, due to its ability to limit contention using RAW groups and slots.

## 7. REFERENCES

- [1] T. Adame, A. Bel, B. Bellalta, J. Barcelo, and M. Oliver. IEEE 802.11ah: the WiFi approach for M2M communications. *IEEE Wireless Communications*, 21(6):144–152, 2014.
- [2] S. Aust and R. V. Prasad. Advances in wireless M2M and IoT: Rapid SDR-prototyping of IEEE 802.11ah. In *IEEE Local Computer Networks Conference*, 2014.
- [3] S. Aust, R. V. Prasad, and I. G. M. M. Niemegeers. Performance study of MIMO-OFDM platform in narrow-band sub-1 GHz wireless LANs. In *11th International Symposium on Modeling & Optimization in Mobile, Ad Hoc & Wireless Networks (WiOpt)*, pages 89–94. IEEE, 2013.
- [4] R. A. Casas, V. Papaparaskeva, R. Kumar, P. Kaul, and S. Hijazi. An IEEE 802.11ah programmable modem. In *IEEE 16th International Symposium on A World of Wireless, Mobile and Multimedia Networks (WoWMoM)*, 2015.
- [5] A. Hazmi, J. Rinne, and M. Valkama. Feasibility study of IEEE 802.11ah radio technology for IoT and M2M use cases. In *2012 IEEE Globecom Workshops*, pages 1687–1692. IEEE, 2012.
- [6] E. Khorov, A. Lyakhov, A. Krotov, and A. Guschin. A survey on IEEE 802.11ah: An enabling networking technology for smart cities. *Computer Communications*, 58:53–69, 2015.
- [7] K. Ogawa, M. Morikura, K. Yamamoto, and T. Sugihara. IEEE 802.11ah based M2M networks employing virtual grouping and power saving methods. *IEICE Transactions on Communications*, E96-B(12):2976–2985, 2013.
- [8] C. W. Park, D. Hwang, and T.-J. Lee. Enhancement of IEEE 802.11ah MAC for M2M communications. *IEEE Communications Letters*, 18(7):1151–1154, 2014.
- [9] M. Park. IEEE 802.11ah: Energy efficient MAC protocols for long range wireless LAN. In *2014 IEEE International Conference on Communications (ICC)*, pages 2388–2393. IEEE, 2014.
- [10] G. Pei and T. R. Henderson. Validation of ofdm error rate model in ns-3. *Boeing Research Technology*, pages 1–15, 2010.
- [11] M. Qutab-ud din, A. Hazmi, B. Badihi, A. Larmo, J. Torsner, and M. Valkama. Performance analysis of IoT-enabling IEEE 802.11ah technology and its RAW mechanism with non-cross slot boundary holding schemes. In *IEEE 16th International Symposium on A World of Wireless, Mobile and Multimedia Networks (WoWMoM)*, 2015.
- [12] O. Raeesi, J. Pirskanen, A. Hazmi, T. Levanen, and M. Valkama. Performance evaluation of IEEE 802.11ah and its restricted access window mechanism. In *IEEE International Conference on Communications Workshops (ICC)*, pages 460–466.
- [13] O. Raeesi, J. Pirskanen, A. Hazmi, J. Talvitie, and M. Valkama. Performance enhancement and evaluation of IEEE 802.11ah multi-access point network using restricted access window mechanism. In *IEEE International Conference on Distributed Computing in Sensor Systems*, pages 287–293, 2014.
- [14] L. Tian, J. Famaey, and S. Latré. Evaluation of the IEEE 802.11ah restricted access window mechanism for dense IoT networks. In *IEEE 17th International Symposium on A World of Wireless, Mobile and Multimedia Networks (WoWMoM)*, Accepted.
- [15] H. Wang. *Supporting Authentication/Association for Large Number of Stations*, 2012., 2012. <https://mentor.ieee.org/802.11/dcn/12/11-12-0112-04-00ah-supporting-of-the-authentication-association-for-large-number-of-stations.pptx>.
- [16] L. Zheng, L. Cai, J. Pan, and M. Ni. Performance analysis of grouping strategy for dense IEEE 802.11 networks. In *2013 IEEE Global Communications Conference (Globecom)*, pages 219–224, 2013.